Slow light in a semiconductor waveguide for true-time delay applications in microwave photonics

Öhman, Filip; Yvind, Kresten; Mørk, Jesper

Published in:
I E E E Photonics Technology Letters

Link to article, DOI:
10.1109/LPT.2007.901435

Publication date:
2007

Document Version
Publisher's PDF, also known as Version of record

Citation (APA):
Öhman, F., Yvind, K., & Mørk, J. (2007). Slow light in a semiconductor waveguide for true-time delay applications in microwave photonics. *I E E E Photonics Technology Letters*, *19*(15), 1145-1147. https://doi.org/10.1109/LPT.2007.901435

Slow Light in a Semiconductor Waveguide for True-Time Delay Applications in Microwave Photonics

Filip Öhman, Kresten Yvind, and Jesper Mørk

Abstract—**We have investigated the slow and fast light properties of a semiconductor waveguide device employing concatenated gain and absorber sections. This letter presents the experimental results as well as theoretical modeling. A large phase shift of 110° and a true-time delay of more than 150 ps are demonstrated. The combination of amplitude and phase control of the modulated signal shows great promise for applications within microwave photonics.**

Index Terms—**Microwave photonics, optical signal processing, semiconductor optical amplifier (SOA), slow light.**

I. Introduction

The possibility of controlling the group velocity of an optical signal has received a lot of attention lately [1]–[7]. The effect has been demonstrated using electromagnetically induced transparency in ultra-cold atomic gases [1] as well as coherent population oscillation (CPO) in a ruby crystal [2] and semiconductor structures [3]–[6]. Slow light effects have been demonstrated both using pulses [1], [6] and sine-modulated signals [2], [4], [5], [7], and are envisioned to have applications within several different areas. One of the more spectacular applications is the possibility to store optical pulses in an all-optical buffer, but theoretical results for the CPO effect [5] indicate that just a few bits can be stored. A less demanding, but very relevant, application is the control of optical microwave signals, where a phase delay of the signal is needed in, for example, optically fed phased array antennas and optical microwave signal processing [8].

We have recently shown that a waveguide device with alternating sections of semiconductor optical amplifiers (SOAs) and electroabsorbers (EAs) can enhance the delay [7] by removing the limitation of the discrete EA originating from the residual absorption [5]. The device can even achieve optical gain [7] with the possibility of independent control of the phase and amplitude of the signal. In this letter, we present the measured and calculated frequency response of the device in order to evaluate the bandwidth of the delay. Furthermore, we investigate the interplay between the amplifying and absorbing sections and demonstrate how to combine their response in order to tailor the complete frequency dependence of the device to achieve a large true-time delay and bandwidth.

Manuscript received February 27, 2007; revised April 12, 2007. This work was supported by the Danish Research Council as well as the European Union through the IST Program QPHOTON.

The authors are with the COM•DTU Department of Communications, Optics and Materials, Nano•DTU, Technical University of Denmark, DK-2800 Kgs. Lyngby, Denmark (e-mail: fo@com.dtu.dk).

Digital Object Identifier 10.1109/LPT.2007.901435

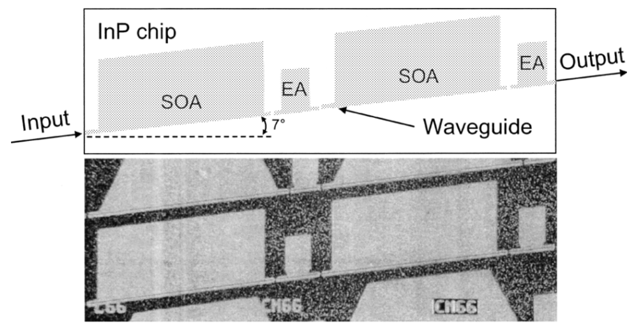

Fig. 1. Photo and schematic of the investigated device. The SOAs and EAs are 545 and 120 μm long, respectively.

II. Device and Model

Two devices have been examined experimentally. They consist of one or two pairs of 545-μm-long SOA and 120-μm-long EA sections; the two-pair device is depicted in Fig. 1.

The phase shift encountered in both SOA and EA sections depends on the power relative to the saturation power [5], which is, hence, important to consider in the design. The device is designed to have a large difference in saturation energy between the SOA and EA, while keeping a fast EA structure. For a given mode-size, the saturation energy is determined by the differential material gain, and in addition for the EA, the screening of the electrical field. Any quantum-confined structure will have a difference in saturation energy between forward and reverse biased sections due to the nonlinear gain versus carrier density relation in these materials. However, using butt-coupling technology, we have further optimized this. The saturation energy for the SOA is increased by using five "deep" quantum wells coupled to a carrier reservoir. This allows operation at high inversion and lowers the material differential gain for the SOA. For the EA, we use 15 more shallow wells which increase the absorption change per volt and ensure fast carrier escape from the wells [9]. The large number of photo excited carriers ensures low saturation energy due to field screening. The actual material compositions are for the SOA: 7-nm $InGa_{0.258}As_{0.86}P$ with $InGa_{0.507}As_{0.86}P$ barrier sandwiched in 140-nm $Q(1.13)$ waveguide, and for the EA: 10-nm-thick $InGa_{0.272}As_{0.757}P$ with $InGa_{0.445}As_{0.757}P$ barrier. A ridge-waveguide structure with BCB planarization and TiO_2–SiO_2AR coatings on 7° angled facets completes the design.

The experiments are performed by sending a sinusoidal intensity modulated light signal through the device under test and measuring the phase and amplitude of the modulated signal relative to a reference beam using a network analyzer [5], [7]. The

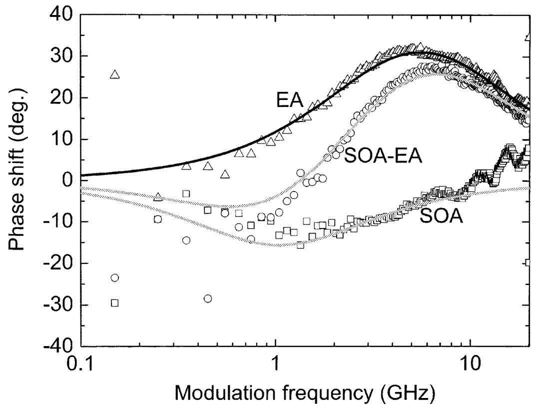

Fig. 2. Measured and calculated phase shift relative the background group index for an SOA-EA pair compared to a single SOA and a single EA.

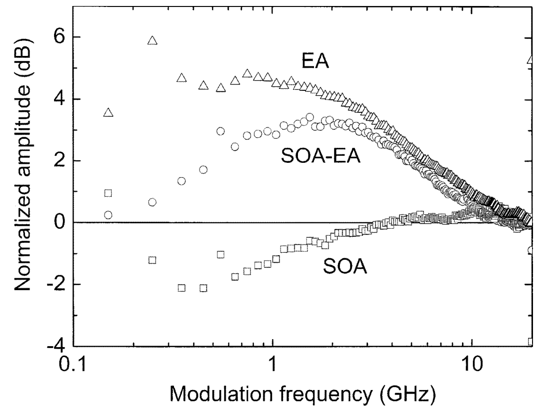

Fig. 3. Measured amplitude normalized to the value at 20 GHz for an SOA-EA pair compared to a single SOA and a single EA.

reference beam has traversed the same path with the device operated at the desired reference point.

The model used in this letter for simulating the device is derived in [5]. In this work, we have extended the model to include multiple sections with absorption or gain. The gain sections model is derived using the same general assumptions as for the absorbers and the main difference is the choice of parameter values. The dependence of the values of the absorption, sweep-out time, and saturation power parameters on reverse bias in the EA has been considered in a phenomenological way [5], valid for low bias voltage [10].

III. Results

As discussed in [3], [6], and [7], the delay in semiconductor devices with an external bias can be both negative and positive, depending on whether the device is biased for gain or absorption. The interplay between the delays in the SOA and the EA in dependence of the modulation frequency is investigated in Fig. 2. The phase shift in one SOA-EA pair as function of modulation frequency is compared to that of an EA section and that of an SOA section. For the measurement on the SOA-EA pair, the phase shift is measured with reference to the background group index achieved by biasing the whole device at transparency. The measurement was then made at input power 5.3 dBm, SOA bias 120 mA, and EA reverse bias 0.7 V. The single SOA and EA sections are measured on the same two-section device by using the proper reference measurements. When measuring the single SOA, the bias to the EA is kept at the reference bias (transparency) and the bias to the SOA was changed to 120 mA. For the single EA, the reference measurement was made with the SOA biased at 120 mA and the EA at transparency, equivalent to subtracting the SOA response from the total SOA-EA response.

The results in Fig. 2 demonstrate that the gain and absorber sections have the opposite responses for the induced microwave phase shift. The two opposite responses can, however, be separated by utilizing the fact that the fast sweep-out time of the carriers in the EA results in a phase shift that reaches maximum at higher frequencies in the EA than in the SOA, which has a longer carrier lifetime. This combined with a design providing an input saturation power in the EA that is lower than the output saturation power of the SOA results in a dominating slow light response from the EA in the component, especially at high frequencies, as seen in Fig. 2.

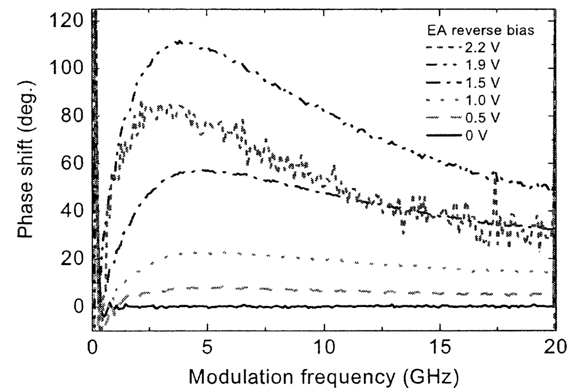

Fig. 4. Measured phase shift for different bias voltages to the two EAs, relative to an EA bias of 0 V. The input power was 5.3 dBm and the bias current 120 mA to each SOA section.

Fig. 3 displays the measured frequency dependence of the amplitude corresponding to the phase shifts in Fig. 2. The amplitude is normalized to the value at the highest frequency (20 GHz) where the response of the device corresponds to the mean gain due to the averaging effect of the relatively slow response times. The amplitude response demonstrates the spectral holes in the gain and absorption created by the CPO effect and seen as an increase in amplitude at low frequencies for the EA and a decrease in the SOA.

In Fig. 4, the measured frequency response of the phase shift in two SOA-EA pairs is displayed. The reference phase is measured at an EA bias of 0 V, input power of 5.3 dBm, and SOA bias current of 120 mA to each section. During the measurement, the power and SOA bias is kept constant while the bias voltage to the two absorber sections is varied. An adjustable phase shift relative to the reference of up to 110° is measured around 4 GHz. At higher frequencies, the limited response time of the device due to a finite carrier lifetime results in smaller phase shifts.

For applications in microwave photonics and in particular phased arrayed antennas, it is important to have a phase shift which depends on modulation frequency as $\Delta\phi(\Omega) = \Delta\phi_0\Omega/\Omega_c$ [8], where Ω_c is the microwave carrier frequency and $\Delta\phi_0$ is the phase shift achieved at this frequency. This translates into a so-called true-time delay which is constant, $\Delta t = \Delta\phi/\Omega$, for the whole signal bandwidth. The

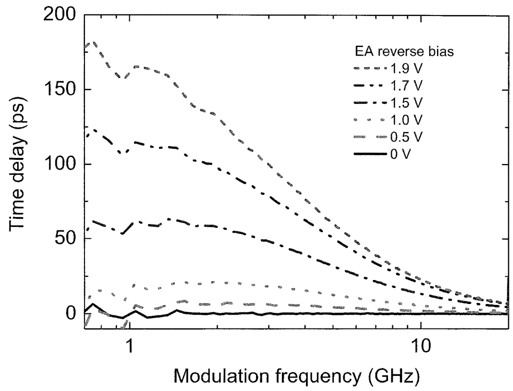

Fig. 5. Measured time delays as function of modulation frequency for different bias voltages to the two EAs.

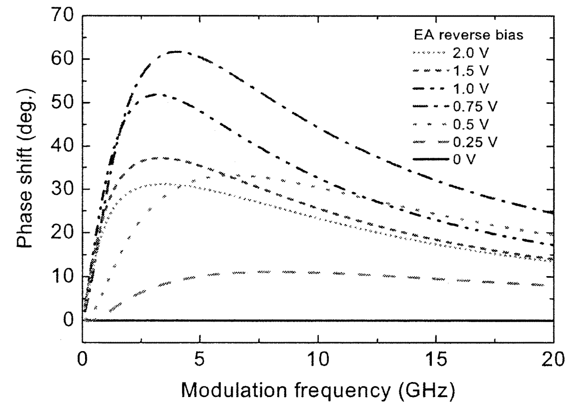

Fig. 6. Calculated phase shift (relative to an EA bias of 0 V) for different values of the bias voltage to the two EAs. The input power was 5.3 dBm.

true-time delay corresponding to the measured phase shift is plotted in Fig. 5. A maximum time delay of 165 ps is measured at low modulation frequency. The time delay falls off rather quickly with modulation frequency resulting in a bandwidth of a few gigahertz.

In the experiments presented in Fig. 4, the reference is chosen at a high input power, large SOA bias current, and zero bias voltage to the EAs. The result is a push–pull effect where the reference is chosen at an operation point where the fast light effect in the SOAs is large and the slow light effect in the EAs is low. As the bias to the EAs is increased, the slow light effect is enhanced while the higher absorption leads to lower input power to the second SOA and, hence, a smaller fast light effect. In total, this gives a relative phase shift in the same direction in both EAs and the second SOA, leading to a larger delay relative to the reference. This operation mode also removes the fast light effect at low modulation frequencies, seen in Fig. 2, and results in the true-time delay in Fig. 5.

In the model [5], the EA and SOA parameters are chosen to give a good fit of the measured phase shift in Fig. 2 and to the measured chip gain (not shown). The input power to the SOA is 5.3 dBm and coupling losses are estimated to 3 dB. The background group index is 3.4 and for the SOAs, the confinement factor is 0.065, the small signal gain coefficient 700 cm^{-1}, the carrier life time 250 ps, and the saturation power is 7 mW. In the EA, the confinement factor is 0.2 and the voltage-dependent parameter values are the small signal absorption coefficient 2176 cm^{-1}, the carrier sweep-out time 77.5 ps, and the saturation power 2.1 mW; all of the values are given at 0.7-V reverse bias. The model shows good agreement with the experiments in Fig. 2. However, when calculating the phase shift for the same conditions as in Fig. 4, only a qualitative agreement is achieved, as seen in Fig. 6. In the model, saturation effects due to the amplified spontaneous emission from the SOAs are not included and neither are the finite reflections at the facets. The model for the EA is based on phenomenological assumptions [5] that do not hold well for large reverse bias [10], which could to some degree account for the discrepancies. Mainly the description of the voltage dependence of the absorption, sweep-out time, and saturation power could benefit from a more detailed model and potentially give a better quantitative agreement.

IV. Conclusion

We have performed experiments and developed a theoretical model to investigate the frequency dependence of slow light in a semiconductor wave guide with alternating gain and absorber sections. The model agrees qualitatively with the experimental results but a more detailed model is required for better quantitative agreement. The investigations demonstrate the feasibility of achieving large true-time delay by cascading several sections and operating in a push–pull mode. The use of alternating gain and absorber sections also give the potential for simultaneous control of the modulation amplitude as well as tailoring of the frequency response. The device thus demonstrates good potential for applications within microwave photonics.

References

[1] L. V. Hau, S. E. Harris, Z. Dutton, and C. H. Behroozi, "Light speed reduction to 17 meters per second in an ultracold atomic gas," *Nature*, vol. 397, pp. 594–598, 1999.

[2] M. S. Bigelow, N. N. Lepeshkin, and R. W. Boyd, "Observation of ultraslow light propagation in a ruby crystal at room temperature," *Phys. Rev. Lett.*, vol. 90, pp. 113903-1–113903-4, 2003.

[3] J. C. Chang-Hasnain and S.-L. Chuang, "Slow and fast light in semiconductor quantum-well and quantum-dot devices," *J. Lightw. Technol.*, vol. 24, no. 12, pp. 4642–4654, Dec. 2006.

[4] P. Palinginis, S. Crankshaw, and F. Sedgwick, "Ultra-slow light (<200 m/s) propagation in a semiconductor nanostructure," *Appl. Phys. Lett.*, vol. 87, p. 171102, 2005.

[5] J. Mørk, R. Kjær, M. van der Poel, and K. Yvind, "Slow light in a semiconductor waveguide at gigahertz frequencies," *Opt. Express*, vol. 13, pp. 8136–8145, 2005.

[6] M. V. D. Poel, J. Mørk, and J. M. Hvam, "Controllable delay of ultrashort optical pulses in a semiconductor quantum dot amplifier," *Opt. Express*, vol. 13, pp. 8032–8037, 2005.

[7] F. Öhman, K. Yvind, and J. Mørk, "Voltage-controlled slow light in an integrated semiconductor structure with net gain," *Opt. Express*, vol. 14, no. 21, pp. 9955–9962, 2006.

[8] I. Frigyes and A. J. Seeds, "Optically generated true-time delay in phased-array antennas," *Trans. Microw. Theory Tech.*, vol. 43, no. 9, pt. 1–2, pp. 2378–2386, Sep. 1995.

[9] R. Y.-F. Yip, P. Desjardins, L. Isnard, A. Aït-Ouali, H. Marchand, J. L. Brebner, J. F. Currie, and R. A. Masut, "Band alignment engineering for high speed, low drive field quantum confined Stark effect devices," *J. Appl. Phys.*, vol. 83, pp. 1758–1769, 1998.

[10] F. Öhman and J. Mørk, "Frequency response of slow and fast light in integrated semiconductor waveguide amplifiers and absorbers," presented at the ECIO 2007, Kgs. Lyngby, Denmark.